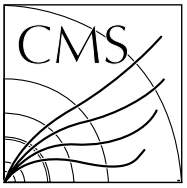

The Compact Muon Solenoid Experiment

CMS Note

Mailing address: CMS CERN, CH-1211 GENEVA 23, Switzerland

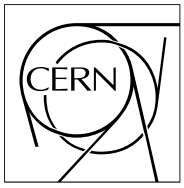

4 April, 2001

Test beam Results of the Forward RPC Prototype Chamber for the CMS Muon Detector

Z. Aftab, H. Hoorani, J.A. Jan, M.S. Khan, T. Solaija

National Centre for Physics, Islamabad, Pakistan.

I. Crotty

CERN, Geneva, Switzerland

Abstract

A full size prototype of the second forward RPC station (RE2/2) for the CMS detector has been tested during the 2000 beam test. The prototype was exposed to high irradiation flux using the CERN Gamma Irradiation Facility (GIF) and the 200 GeV muon beam from X5 beamline. We have studied number of chamber parameters which are relevant for the trigger such as: time resolution, efficiency, cluster size and rate capability. We have used two different gas mixtures to understand the effect of SF_6 on the efficiency plateau and the rate capability of the chamber. We have also studied the intrinsic chamber rate for different discrimination thresholds.

1 Introduction

The Resistive Plate Chambers (RPCs) are the part of the CMS muon detector. An RPC consists of two parallel plates, made out of phenolic resin (bakelite) with a bulk resistivity of 10^9 - 10^{10} Ωcm, separated by a gas gap of a few millimeters. The whole structure is made gas tight. The outer surfaces of the resistive material are coated with conductive graphite paint to form the HV and ground electrodes. The readout is performed by means of aluminium strips separated from the graphite coating by an insulating PET film.

Due to their fast response time and the good time resolution, the RPCs have been chosen as dedicated detectors for the first level muon trigger system [1]. These detectors will work under very high background conditions. In particular the background flux in the forward region due to low energy photons (up to about 100 MeV) will reach the level of $10^5 \mathrm{cm}^{-2}\mathrm{s}^{-1}$. In the past, RPCs have been operated in streamer mode [2]. However, the rate capability obtained in such operational conditions is limited ($\approx$ 100 Hz/cm^2) and it is not adequate for LHC. This situation can be improved by operating the detector in the so-called avalanche mode [3, 4, 5]. In the avalanche mode the applied field across the gap is reduced by lowering the applied voltage. This reduces the charge collected by electrodes and requires more amplification. By using more than one gap and the single readout strips one can increase the total charge collected. The CMS Collaboration has adopted double gap RPCs as their baseline. In addition, the R&D results obtained during the last few years [6, 7, 8, 9] show that the rate capability of RPCs can be improved by using the bakelite of low resistivity.

In September 2000, a full size prototype of the RE2 type double gap RPC chamber for CMS was tested at the CERN Gamma Irradiation Facility (GIF). In this technical note, we present the results of the data collected using the above prototype.

2 Experimental Setup

In order to maintain projectivity, the chamber shape is trapezoidal. The chamber dimensions were 1676 mm (length), 609 mm (narrow side) and 901 mm (wide side). The thickness of the fully assembled chamber was around 36 mm. It covers 10° in ϕ and three η segments corresponding to $\Delta\eta \approx 0.57$. We have used three gas gaps made by the General Technica to built the chamber. For the gas gaps phenolic bakelite is used with a resistivity of 7 x 10^9 Ωcm. We have assembled the chamber using the design of double gap RPCs and the width of each gas gap was 2 mm. For the readout trapezoidal strips were used. The average strip width was around 2.5 cm. There were 32 strips per η segment [10]. For the readout electronics we have used the VLSI supplied by the Bari group. The VLSI was designed and manufactured in 0.8 μBiCMOS technology. The charge sensitivity of amplifier was 2 mV/fC and the nominal discrimination threshold was set to 87.5 fC (175 mV). A total of 96 readout channels were available whereas we have only read the 64 channels in the high η region. The signals from the readout electronics were fed in to a multi-hit TDC (LeCroy 2277) with a 64 μs gate and 1 ns sensitivity. The TDC was set in the common stop mode. The chamber was tested with two different gas mixtures one with SF_6 and the other without SF_6. The gas mixtures used were 97.5% $C_2H_2F_4$, 2.5% iso-C_4H_{10} and 95.7% $C_2H_2F_4$, 3.5% iso-C_4H_{10} and 0.6% SF_6.

The chamber was placed 2.3m away from the Gamma source which produces the photon flux of 661 keV using a 20 Ci ^{137}Cs source. A system of lead filters, that can be moved in front of the source, allows to reduce the flux up to a factor of 10000. The tests were performed with absorption 1 (ABS 1, i.e. no filters), absorption 2, 5 and 10 (ABS 2, ABS 5 and ABS 10 i.e. nominal absorption factors 2, 5 and 10 with respect to ABS 1) and with source off. A system of scintillators (in fact two scintillators one small and the other one big) was used to trigger on the beam particles. The chamber was located downstream of X5 beam line of the CERN SPS ring. The beam consisted of muons with an energy of 200 GeV. The beam particles from the X5 beam were tagged by two wire Beam Chambers (BCs) having a spatial resolution of less than 200 μm.

3 Data Analysis

To account for the different temperature and pressure during data taking, the applied voltage is normalized at the reference values T_0=293 K and P_0=1000 mbar. The data from TDCs have been used to study the different chamber parameters under different irradiation fluxes. In Fig. 1, the measured dark currents are shown for the single gap. At the nominal value of applied voltage dark currents are 70 μA/m^2 and 270 μA/m^2 for the source off and source on with ABS 1 respectively. In Fig. 2, we show the time resolution of one particular channel under two different conditions namely: with gamma source off and with gamma source on at ABS 1. There is some degradation in the case when the source is on at ABS 1. In Fig. 3, the mean arrival time for different applied voltages and different

source conditions (no source, ABS 1, ABS 2, and ABS 5) is shown. The mean arrival time is defined by time of median strip in the cluster with respect to the trigger generated by the beam.

In Fig. 4, typical efficiencies for different source conditions are shown. The number were obtained by using the hits within a 20 ns time window centred at the mean arrival time of the fastest strip. The efficiency is maximum as expected when the source is off and the typical value is around 99%. For the case, ABS 1, we observe lower values i.e. around 96%. From this figure, one can see that the usable size of efficiency plateau for all source intensities of the photon flux is approximately 400 V and the plateau starts around 9.0 kV. We have also taken data by changing the discrimination threshold. We have scanned at three different values 150 mV (75 fC), 175 mV (87.5 fC) and 200 mV (100 fC) with two different source conditions i.e. no source and source with ABS 1. The results are shown in figure 5. One can see the drop in the efficiency with increasing discrimination threshold.

In Fig. 6, percentage of spurious hits are shown at different applied voltages and for different source intensities. A hit is defined as spurious if it is 100 ns out of the mean arrival time of the fastest strip. For the case when the gamma source is off, spurious hits are less than one percent. For the case when the gamma source is on with the maximum intensity (ABS 1), in the worst case where applied voltage is 9.6 kV spurious hits are around 12%.

In Fig. 7, the mean cluster sizes are shown for different photon fluxes. To define a cluster, we first ordered in time all the signals and then searched for the clusters. A cluster was defined by grouping adjacent strips with signals inside a Δt=20 ns time window. We show the mean cluster size in muon triggered events and in random triggered events. We have estimated the chamber counting rate by using the clusters. Time difference between random events are well described by an exponential distribution characterized by a probability density function:

$$f(t) \; = \; a \; exp(-at) \tag{1}$$

where t is the time and a represents the average rate at which events are occurring. In our case, we have used the time difference between two clusters. In Fig. 8, time difference between two consecutive clusters over 32 strips with ABS 1 are shown. The slope of the curve in figure (8) gives directly the overall counting rate (in ns^{-1}). We estimate a rate of 800 Hz/cm^2 averaged over the 32 strips area under the maximum flux from the gamma source (ABS 1) with applied voltage of 9.2 kV. In Fig. 9, the chamber counting rate is shown for different applied voltages and under different source conditions. The rates are calculated outside the muon beam time window. One can see from figure 9 that the chamber counting rate is lowest when the Gamma source is off and the highest when the Gamma source is on with ABS 1. In addition, in figure 10 we show the rates at different discrimination thresholds with the source at ABS 1.

We have also used another gas mixture for studying the chamber. This gas mixture included 0.6% SF6. In the figure 12, efficiency curves are shown for different values of discrimination threshold versus the applied voltage. In this case, the efficiency plateau is shifted by 0.8 kV towards higher values of applied voltage.

We have also studied the effect of different discrimination threshold settings on the rates where the gamma source was off. Figures 11 and 13 show this behaviour versus the applied voltage with and without SF6. One can see from these figures that lower the discrimination threshold higher the rates as expected.

4 Discussion and Conclusions

In figure 2, the distribution of the signal arrival times is shown at 9.2 kV with two different source conditions i.e. source off and source on with ABS 1. For both cases we have fitted Gaussian with σ = 1.08 ns and σ = 1.24 ns and the base is within 20 ns. The mean arrival time for the median strip in the cluster is shown in the figure 3. The efficiency of the chamber to detect beam particles is shown in figure 4 as a function of applied voltage. The efficiency is defined as follows:

$$\epsilon \; = \; [(N_{ob}/N_t) - P_s]/(1 - P_s) \tag{2}$$

where N_{ob} is the number of observed events in a given time window, N_t is the number of triggers and P_s is the probability that a spurious hit appears in the chamber and ϵ is the RPC efficiency. The probability of the spurious hit P_s is determined by counting the hits in a time window delayed 100 ns after the trigger.

Currently, within CMS the effect of intrinsic noise of the RPCs on the level-1 muon trigger was discussed [11]. This study has shown that for the reasonable trigger rates and efficiency, the intrinsic noise of the RPCs should be kept below 20 Hz/cm^2. To understand the problem better, one should note that the total allowed trigger rate at

level-1 is 30 kHZ which is shared by the level-1 muon trigger and the calorimetric trigger. For the level-1 muon trigger, allowed rate is 15 kHz where more than 50% of the trigger rate is due to single muon trigger. This study shows that for acceptable trigger efficiency and for the reasonable trigger rates RPCs are required to achieve the following:

$$\epsilon_{RPC} \geq 97\%, \ \sigma_{RPC} \leq 3\,ns, \ \mathrm{R}ate = 20\,Hz/cm^2 \tag{3}$$

Keeping the above issue in mind we show several plots related to the chamber rate capability. In figure 9, the chamber rates are shown for different values of applied voltages and under different source conditions. In this case, the discrimination threshold was set to the nominal value of 87.5 fC(175 mV) and the gas mixture used has no SF_6. At the nominal value of the applied voltage (9 kV), the chamber rates are 40 Hz/cm^2 and 800 Hz/cm^2 for the condition when the source is off and when the source is on with ABS 1 respectively. With the same gas mixture and the gamma source at maximum flux (ABS 1), we did a threshold scan by changing the discrimination threshold from 150 to 200 mV. As shown in Fig. 10, with the discrimination threshold of 150 mV at the nominal value of the applied voltage we measure a rate of 1400 Hz/cm^2 and for 200 mV we measure 1000 Hz/cm^2. For the case when the source is off, we measure at 9.0 kV the chamber rates of 50 Hz/cm^2 and 20 Hz/cm^2 for threshold values of 150 mV and 200 mV respectively. We have also performed a discrimination threshold scan with a gas mixture containing SF_6. For the lowest (125 mV) and the highest (225 mV) values we measure the chamber rate of 130 Hz/cm^2 and 30 Hz/cm^2 respectively at nominal applied voltage (9.0 kV).

In conclusion, we can say that the prototype built has performed well. Using the chamber we were able to measure number of important parameters which are relevant to understand the chamber performance and their effects on the level-1 muon trigger. The study of chamber intrinsic noise shows that one can improve it by increasing the discrimination threshold but this will affect the efficiency of the chamber.

Acknowledgement

We would like to thank H. Reithler and his staff for providing DAQ system and some of the necessary hardware. We would also like to thank the Bari group for their help and technical assistance, in particular G. Iaselli and A. Colaleo.

References

[1] Technical Design Report, CERN/LHCC 97-32.

[2] R. Santonico and R. Cardarelli, Nucl. Instr. and Meth. 187 (1981)377-380.

[3] R. Cardarelli et al., Nucl. Instr. and Meth. A333 (1993)399.

[4] I. Duerdoth et al., Nucl. Instr. and Meth. A348 (1994)303.

[5] C. Bacci et al., Nucl. Instr. and Meth. A352 (1995)552.

[6] M. Abbrescia et al., Nucl. Instr. and Meth. A417 (1998)16.

[7] M. Abbrescia et al., Nucl. Instr. and Meth. A414 (1998)135.

[8] H. Czyrkowski et al., Nucl. Instr. and Meth. A419 (1998)490.

[9] M. Abbrescia et al., Nucl. Instr. and Meth. A409 (1998)43.

[10] Z. Aftab et al., "Geometrical Layout and Mechanical details of CMS End Cap RPC.", CMS Internal Note.

[11] For details see the talk by Giacomo Bruno http://www.pv.infn.it/ bruno/cmsweek9-2000.pdf

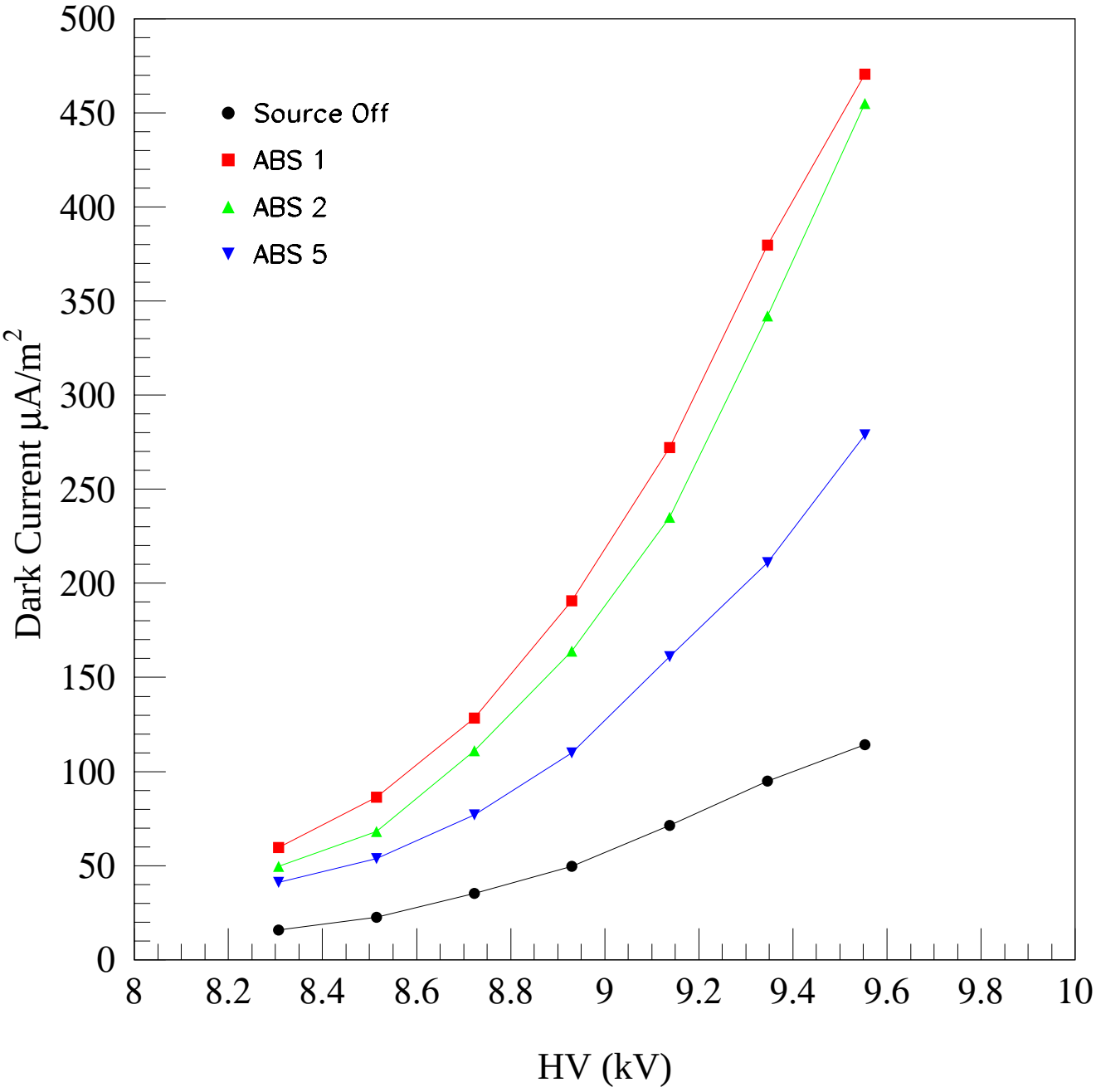

Figure 1: The measured dark currents of a single gap are shown for different applied voltages with different source condition: source off, ABS 1, ABS 2 and ABS 5.

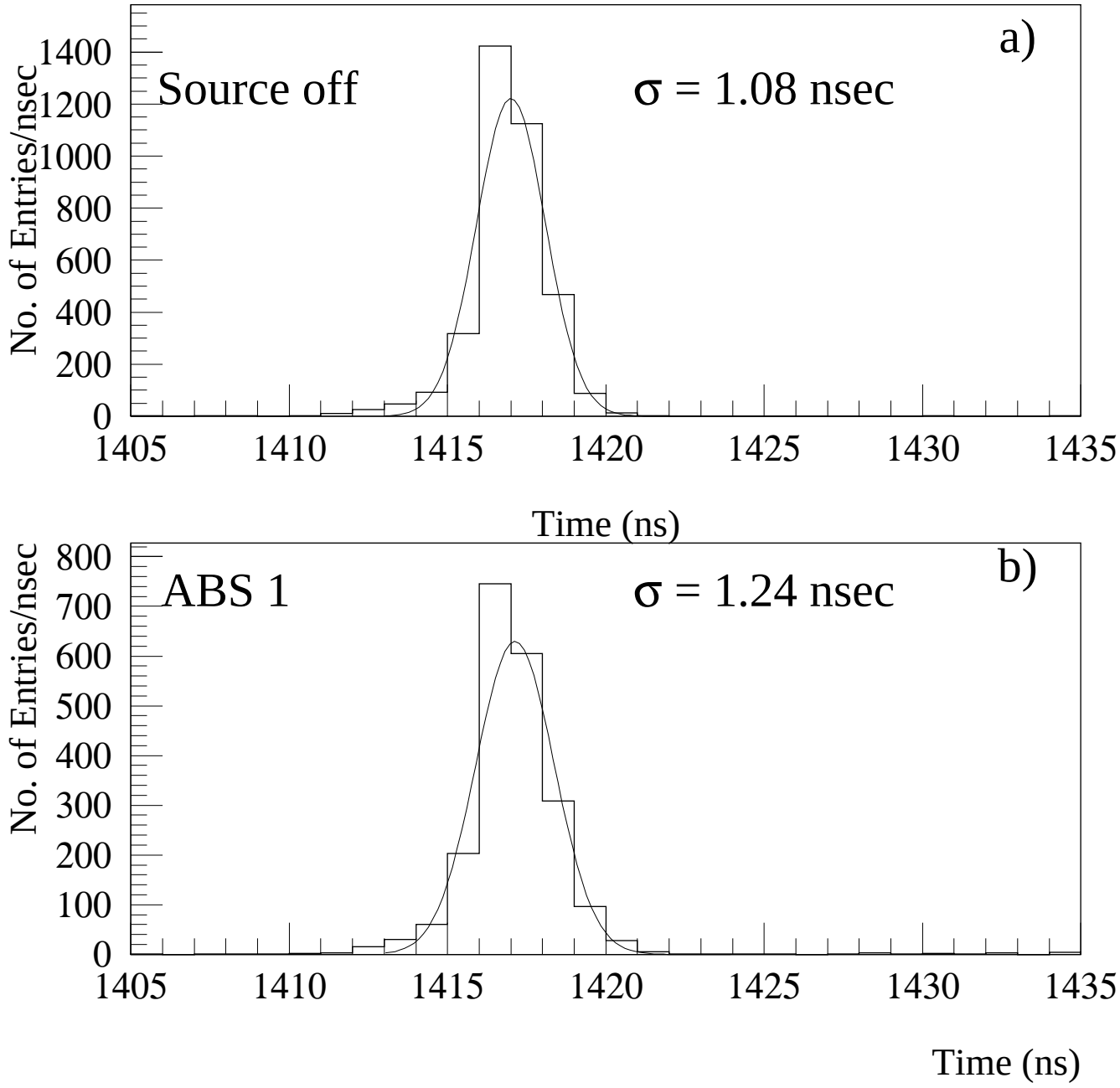

Figure 2: The time response of the chamber at 9.0 kV under two different source conditions: a) gamma source off, b) gamma source on with maximum flux.

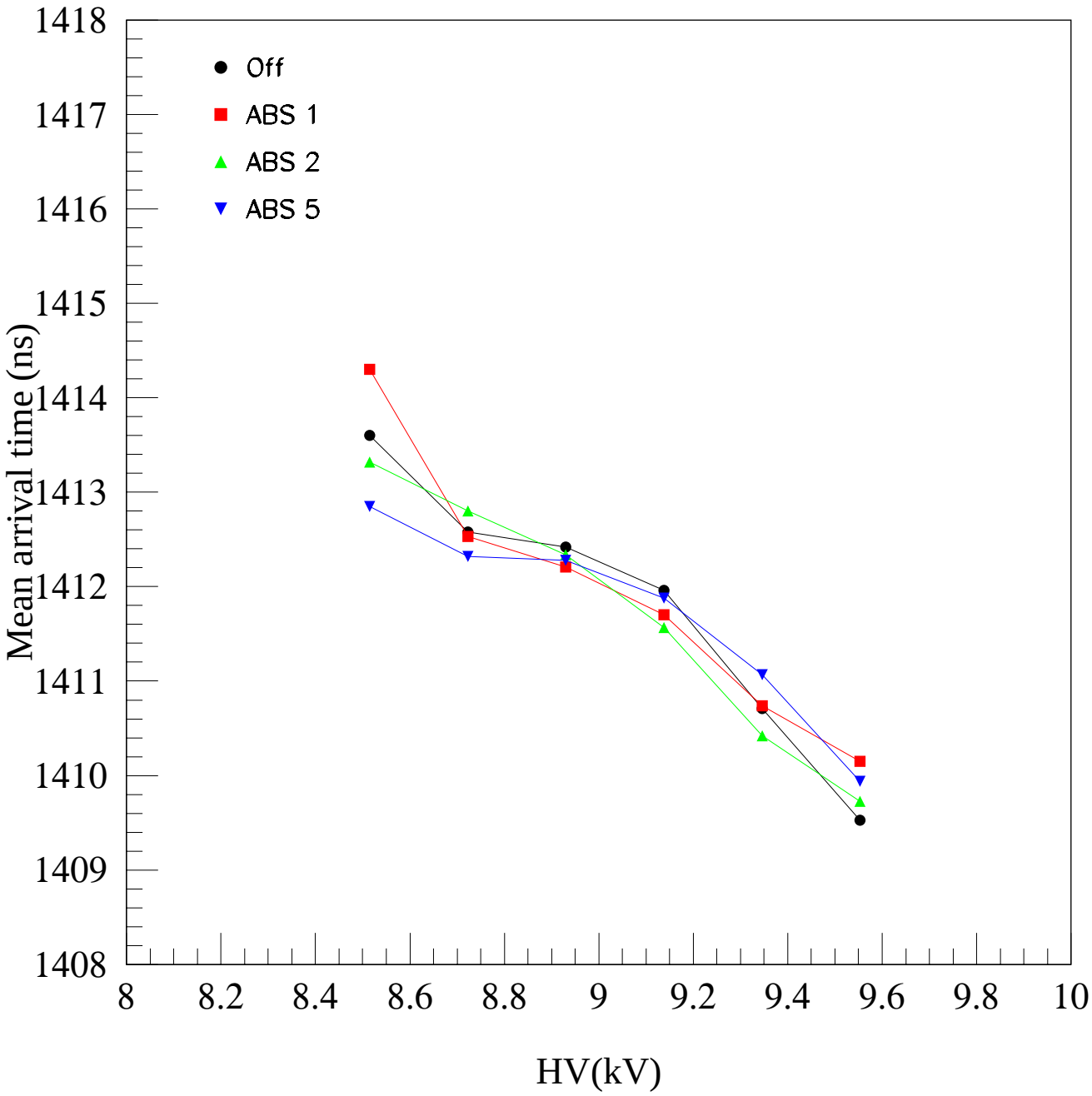

Figure 3: The mean arrival time defined using the time of the median strip in a cluster.

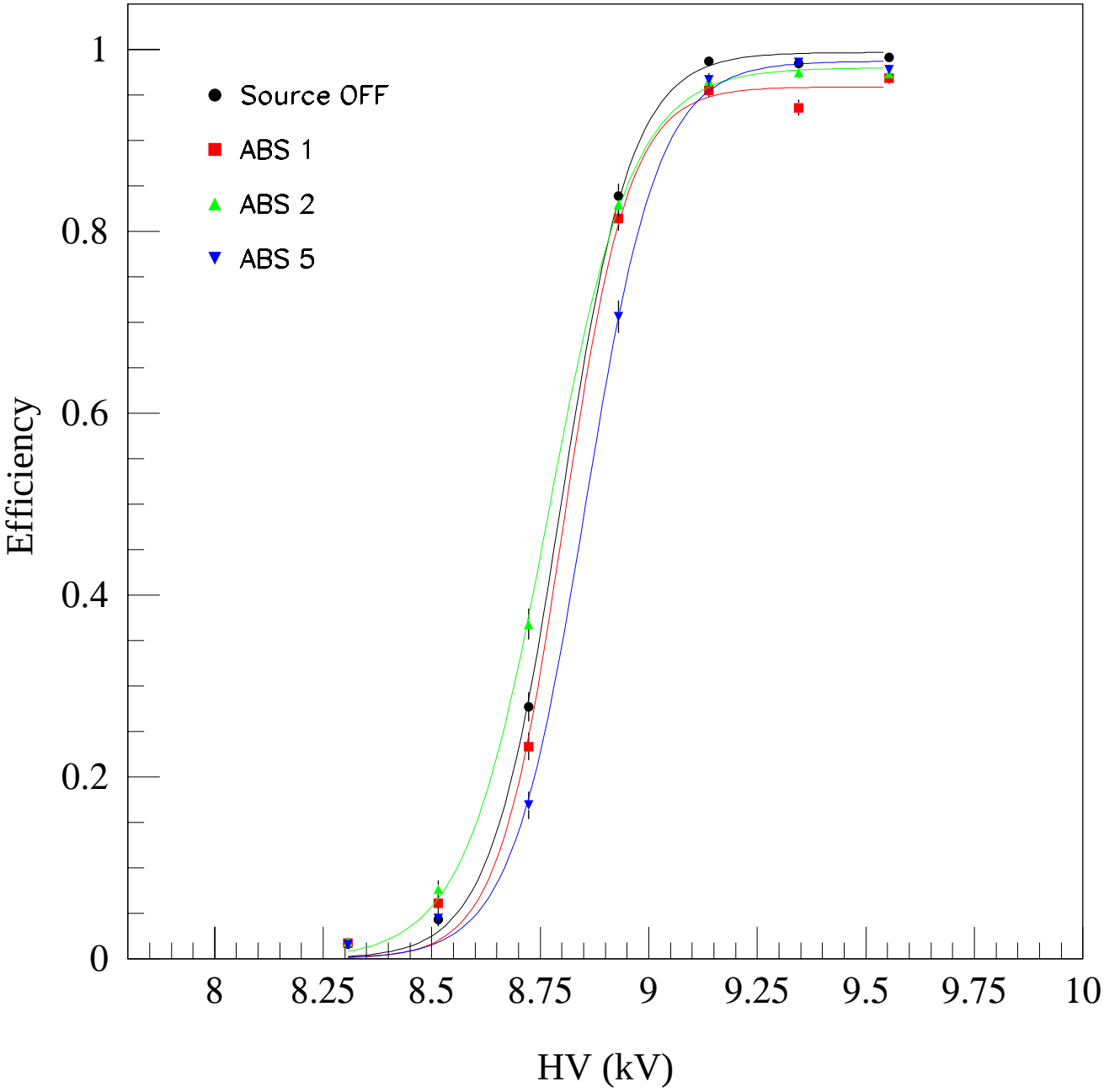

Figure 4: The chamber efficiencies for different photon flux intensities namely: source off, ABS 1, ABS 2 and ABS 5. In all cases the plateau is reached around 9 kV.

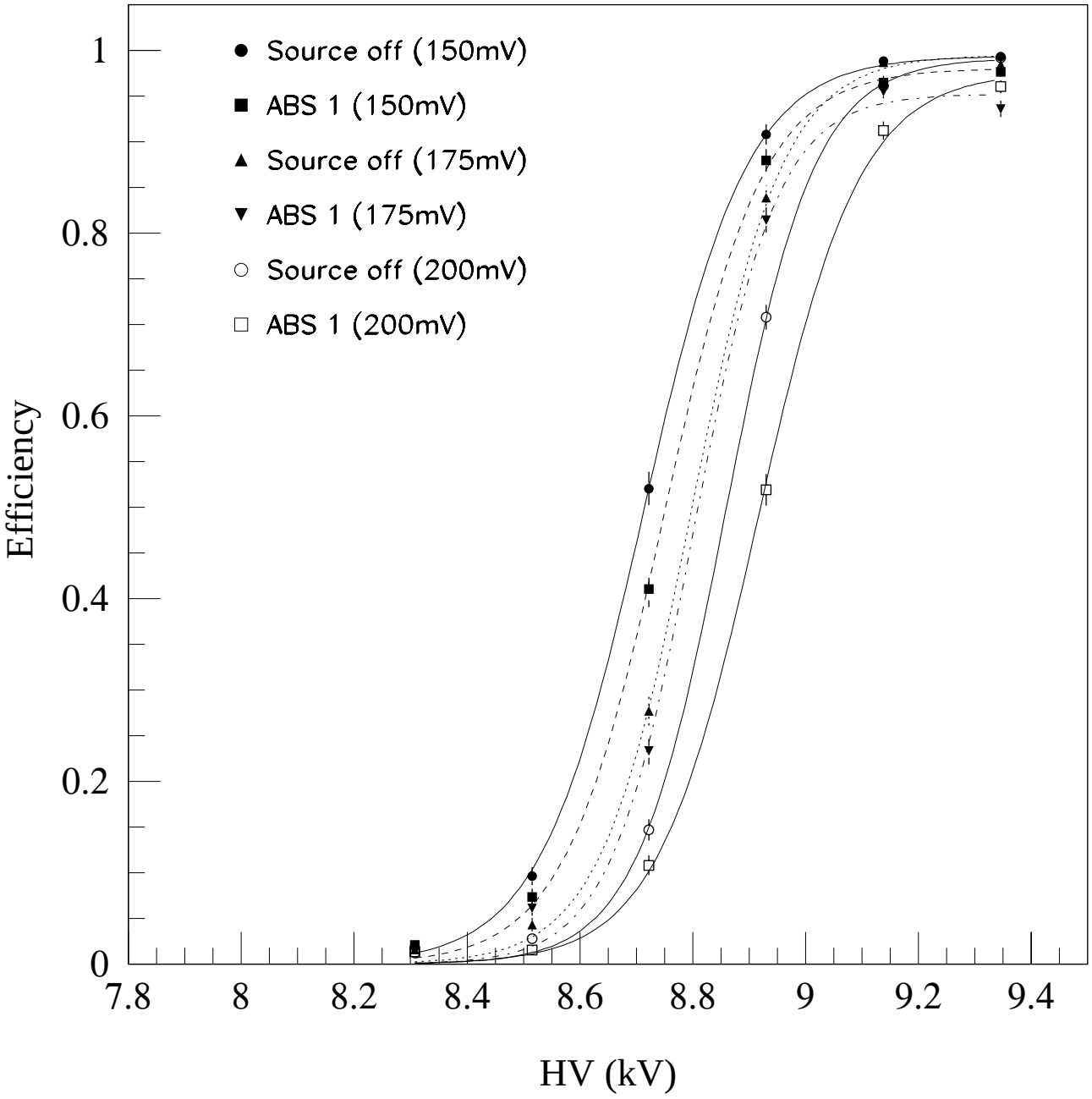

Figure 5: The chamber efficiencies for different discrimination thresholds under different irradiation conditions are shown.

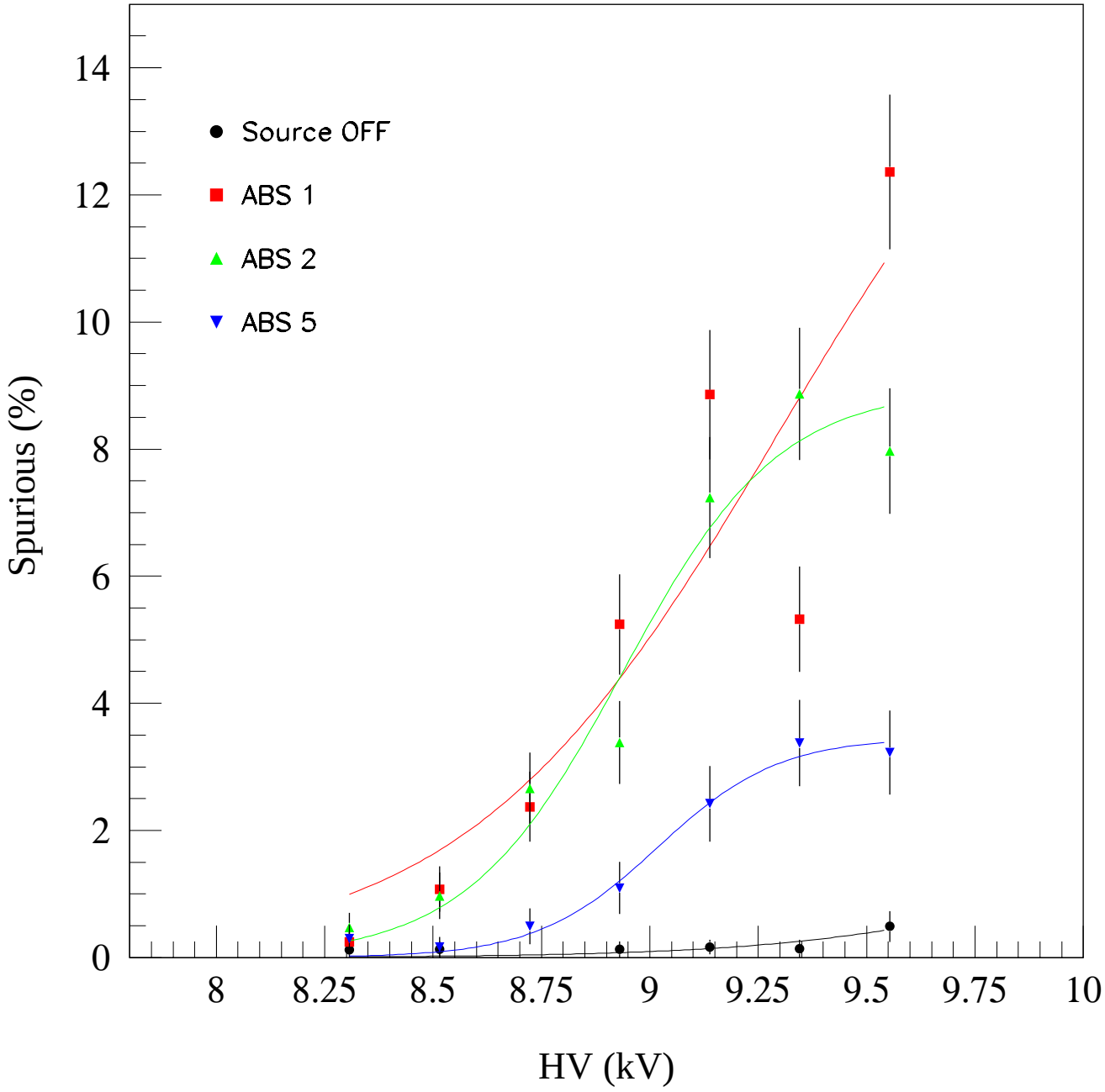

Figure 6: The percentages of spurious hits defined in the text are shown for different photon flux intensities namely: source off, ABS 1, ABS 2 and ABS 5.

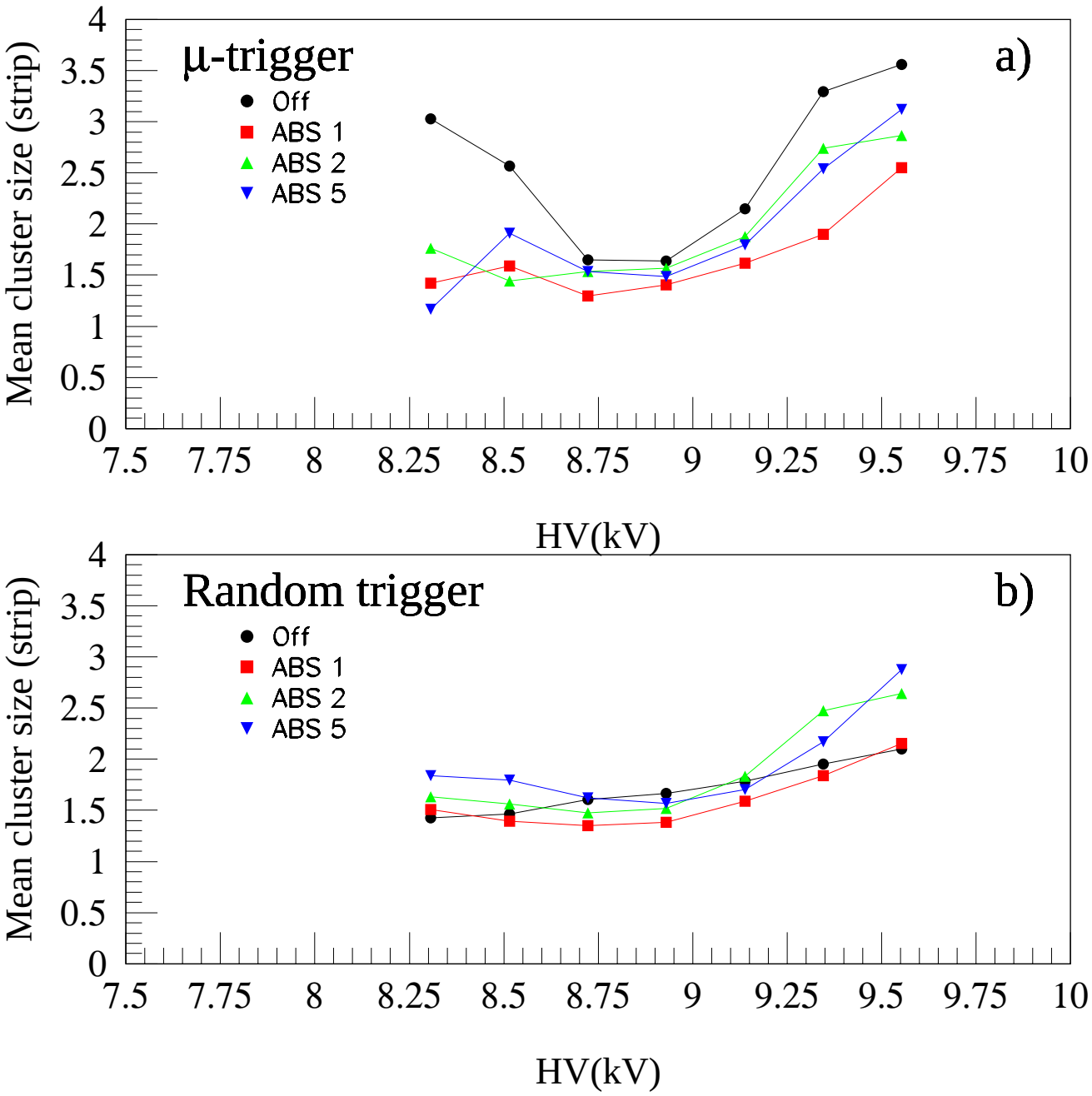

Figure 7: The mean cluster sizes at different high voltages and source conditions. The sizes are shown under two conditions namely: a) for events which are triggered by the beam particles, b) for events where trigger is generated randomly.

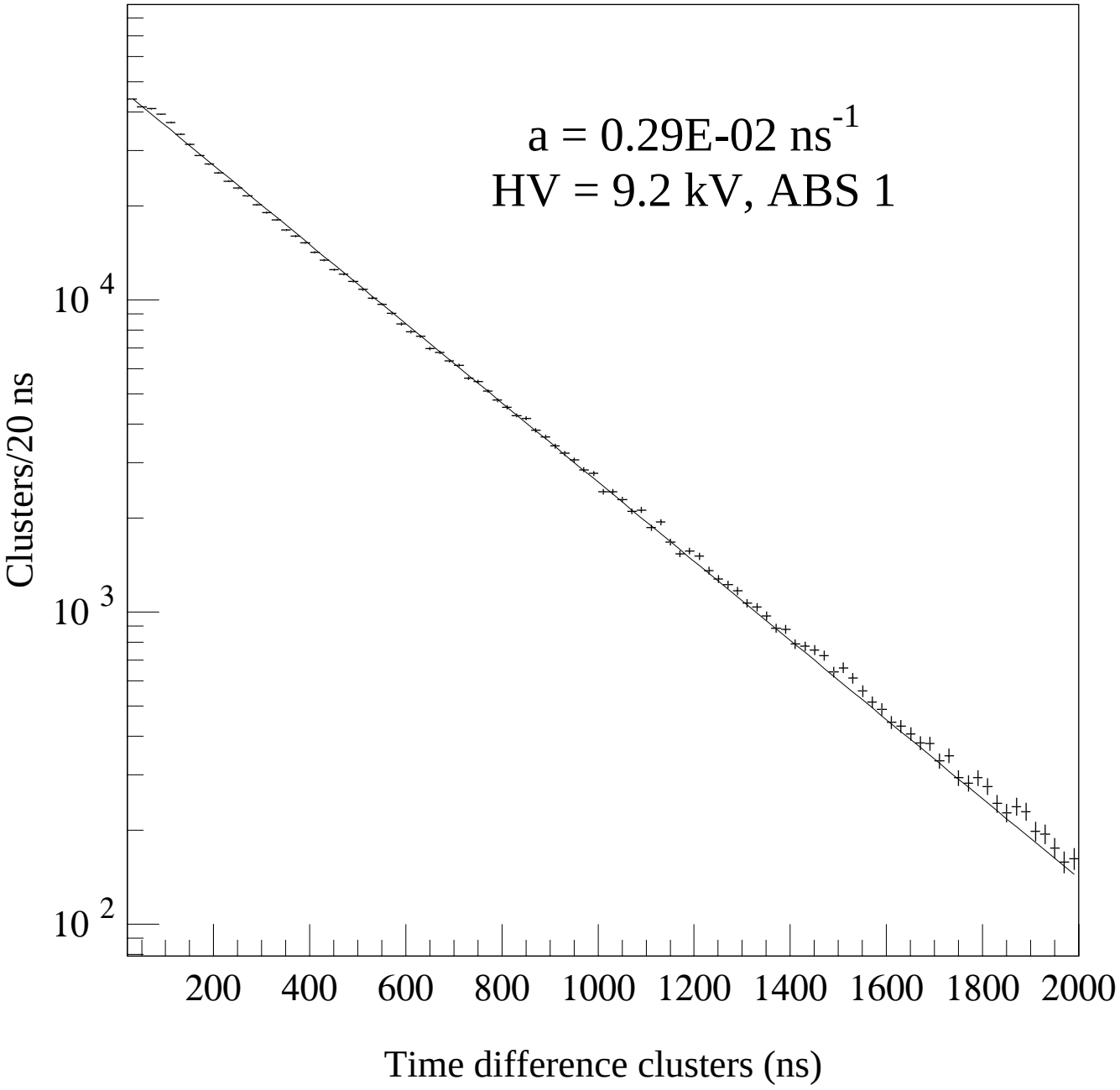

Figure 8: Time difference between two consecutive clusters at 9.2 kV and at ABS 1. The straight line fit gives the slope of the curve which corresponds to the parameter a, which is defined in the text.

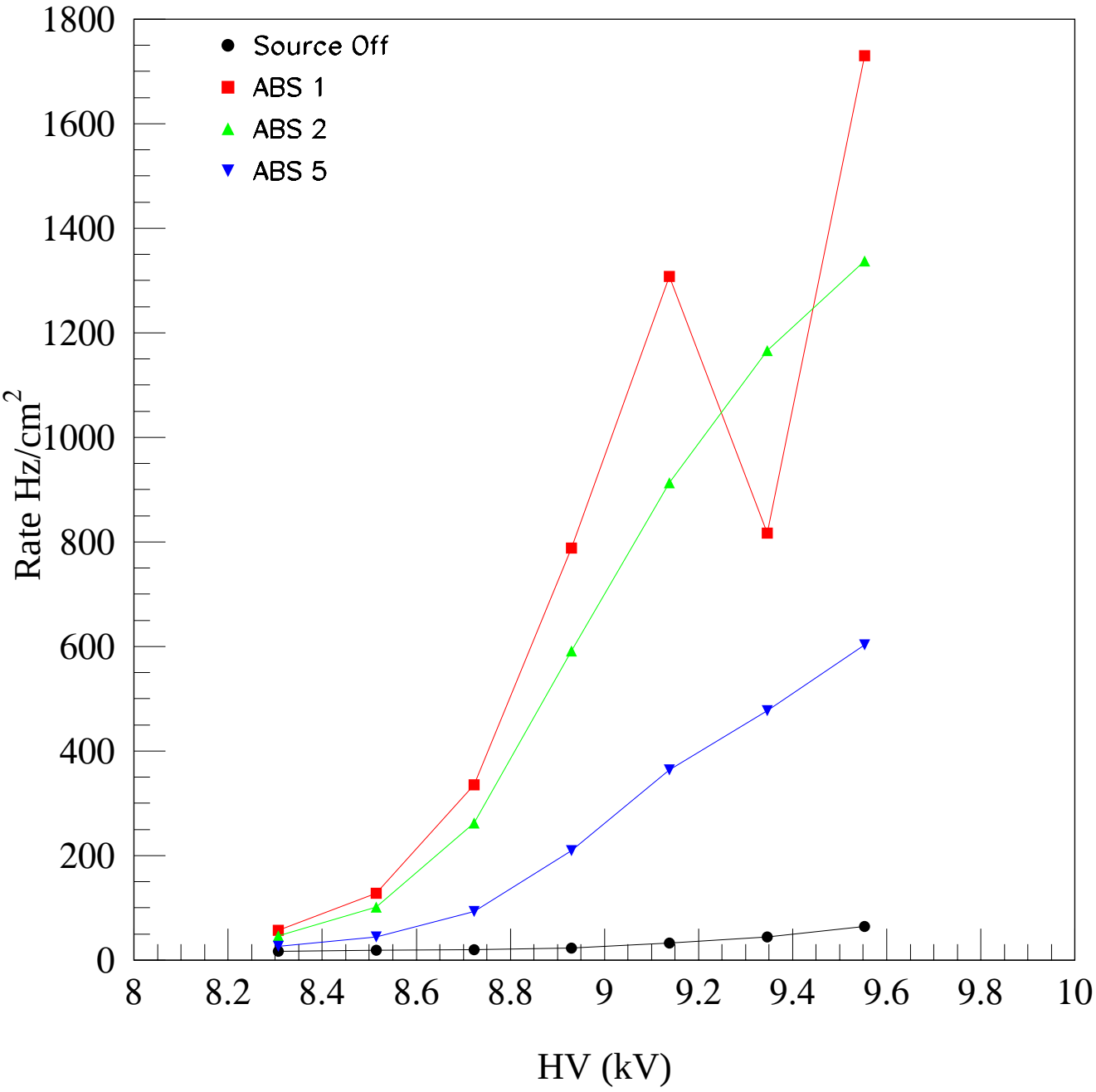

Figure 9: The chamber counting rate is shown at different applied voltage and with four different irradiation conditions namely: no source, ABS 1, ABS 2 and ABS 5.

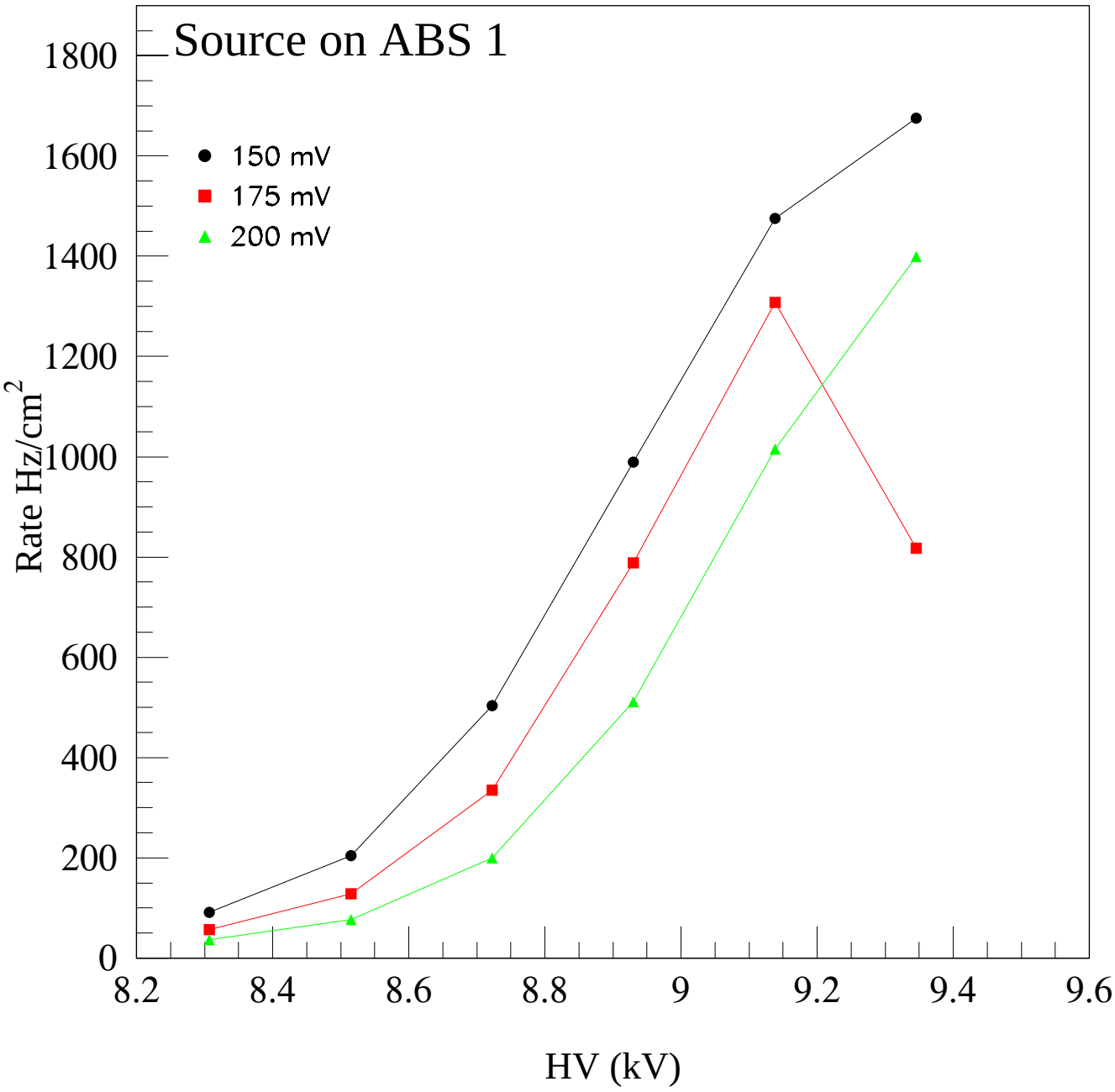

Figure 10: The chamber counting rate is shown at different applied voltage and for different values of discrimination threshold with source on at ABS 1.

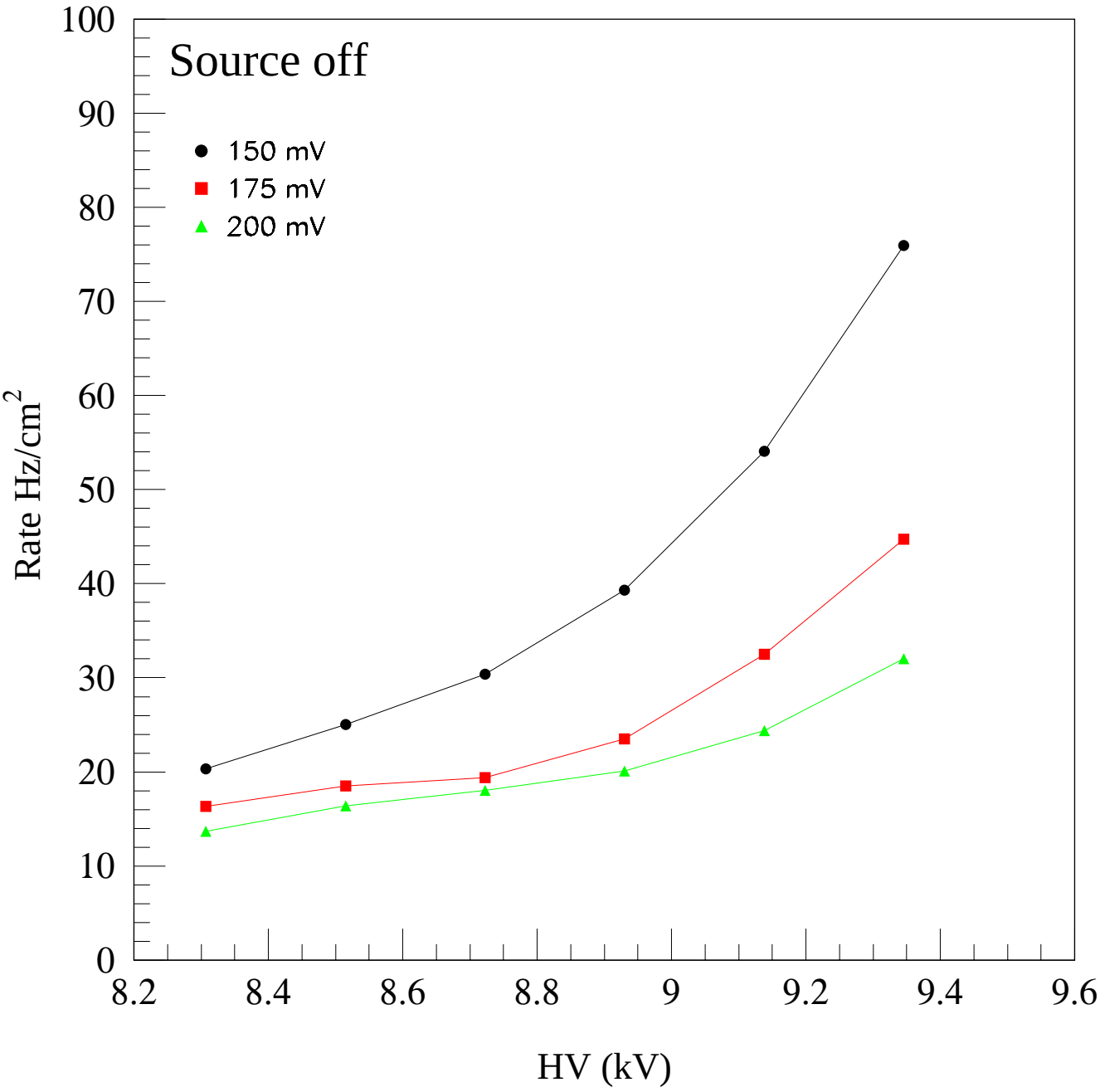

Figure 11: The chamber counting rate is shown for different discrimination thresholds at different applied voltages without SF6 and the gamma source turned off.

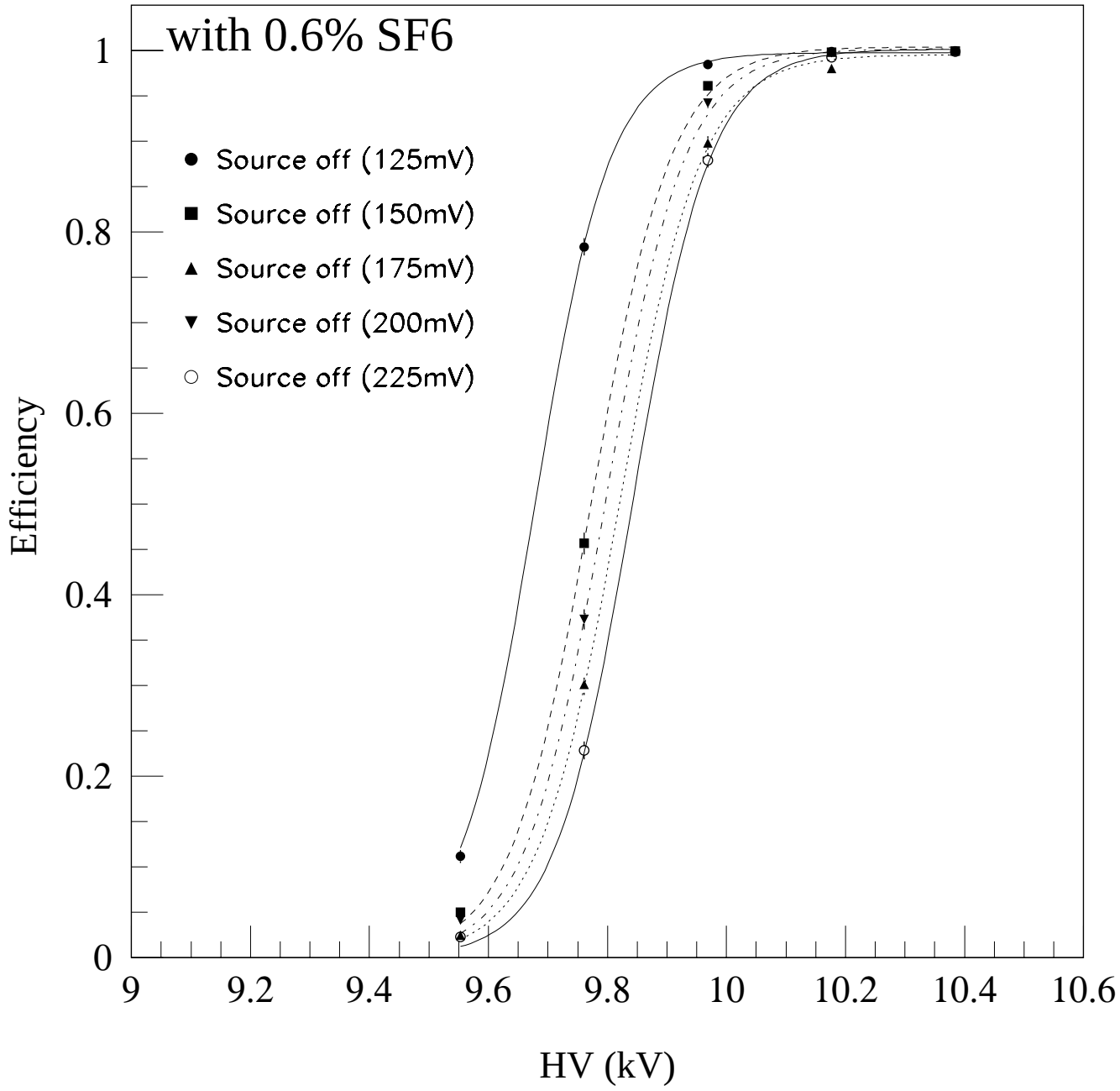

Figure 12: Efficiency curves are shown for different discrimination thresholds at different applied voltages with SF6 and the gamma source turned off.

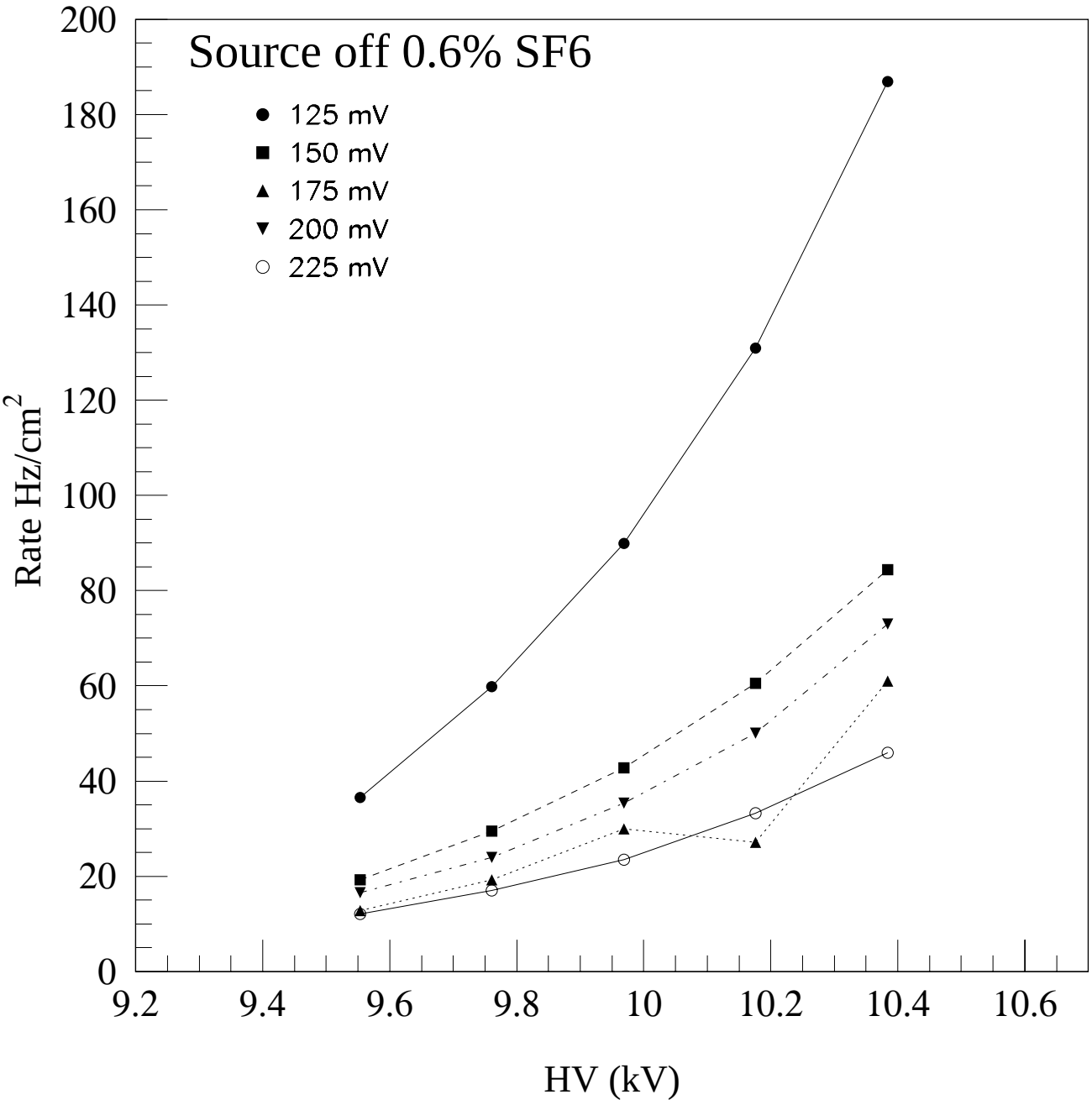

Figure 13: The chamber counting rate is shown for different discrimination thresholds at different applied voltages with 0.6% SF6 and the gamma source turned off.